Structure of singly terminated polar $DyScO_3$ (110) surfaces

J. E. Kleibeuker, B. Kuiper, S. Harkema, D. H. A. Blank, G. Koster,* and G. Rijnders
Faculty of Science and Technology and MESA + Institute for Nanotechnology, University of Twente, 7500 AE Enschede, The Netherlands

P. Tinnemans and E. Vlieg
Radboud University Nijmegen, Institute for Molecules and Materials, 6525 AJ Nijmegen, The Netherlands

P. B. Rossen
Department of Materials Science and Engineering, University of California, Berkeley, California 94720, USA

W. Siemons
Material Science and Technology Division, Oak Ridge National Laboratory, Oak Ridge, Tennessee 37831, USA

G. Portale
Netherlands Organization for Scientific Research (NWO), DUBBLE at ESRF, 38043 Grenoble Cedex, France

J. Ravichandran
Applied Science and Technology graduate group, University of California, Berkeley, California 94720, USA and Materials Sciences Division, Lawrence Berkeley National Laboratory, Berkeley, California 94720, USA

J. M. Szepieniec
Faculty of Science and Technology and MESA + Institute for Nanotechnology, University of Twente, 7500 AE Enschede, The Netherlands and Department of Physics, University of California, Berkeley, California 94720, USA

R. Ramesh
Department of Physics, University of California, Berkeley, California 94720, USA, Department of Materials Science and Engineering, University of California, Berkeley, California 94720, USA, and Materials Sciences Division, Lawrence Berkeley National Laboratory, Berkeley, California 94720, USA

(Received 21 November 2011; revised manuscript received 21 March 2012; published 6 April 2012)

We have studied the polar surface of singly terminated $DyScO_3$ (110) crystals by reflective high-energy electron diffraction, surface x-ray diffraction and angle-resolved mass spectroscopy of recoiled ions. These techniques show that the surfaces are (1×1) reconstructed, which points to the absence of ordered cation vacancies at the surface. The best surfaces were obtained after a selective chemical wet etch. We suggest that for ScO_2 terminated surfaces, adsorbates, or oxygen vacancies are most likely to occur in order to overcome the polarity difference between stoichiometric bulk crystal and vacuum.

DOI: 10.1103/PhysRevB.85.165413 PACS number(s): 68.47.Gh, 61.05.jh, 61.05.cp, 68.49.Jk

I. INTRODUCTION

Orthorhombic $DyScO_3$ is a paramagnetic insulator with a pseudocubic (pc) lattice parameter of 0.395 nm at room temperature.[1,2] $DyScO_3$ substrates are of high interest for studies on strain effects and oxygen octahedron rotations in oxide heterostructures.[3–6] In the $[001]_{pc}$ direction, the crystal structure can be seen as a stack of alternating DyO and ScO_2 planes. Using these substrates for controlled growth of epitaxial heterostructures with atomic precision, atomically flat surfaces with single termination are crucial. Several studies have shown that singly terminated perovskite-type oxide surfaces can be achieved by chemical etching, as reported for, e.g., $SrTiO_3$ (TiO_2 terminated) and $DyScO_3$ (ScO_2 terminated).[7–9]

Comparing $SrTiO_3$ and $DyScO_3$ atomic planes in the $[001]_{pc}$ direction, a crucial difference between the two crystals is present. $SrTiO_3$ consists of alternating neutral planes of SrO and TiO_2, while the DyO^+ and ScO_2^- planes of $DyScO_3$ are charged. A singly terminated and bulklike $DyScO_3$ surface will result in a polar discontinuity at the surface, independent of DyO or ScO_2 termination, which is energetically unfavorable. Therefore a surface reconstruction is likely to occur. This could result from, e.g., oxygen or cation vacancies, ion displacement, electronic reconstruction, and adsorbates. Determination of the type of reconstruction can aid in optimization of complex oxide film growth on these surfaces.[10] Many studies have focused on reconstructions of polar perovskite surfaces, experimentally as well as theoretically, see, for example, Refs. 11–14. However, to our knowledge, possible reconstructions of singly terminated polar $(001)_{pc}$ perovskite-type oxide substrate surfaces have not been studied experimentally.

In this paper, we will discuss the surface structure of polar perovskites, using the results of several surface sensitive techniques: atomic force microscopy (AFM), reflection high-energy electron diffraction (RHEED), surface x-ray diffraction (SXRD), and angle-resolved mass spectroscopy of recoiled ions (AR-MSRI). These techniques are all very sensitive to the top-most surface layer. AFM gives information on the

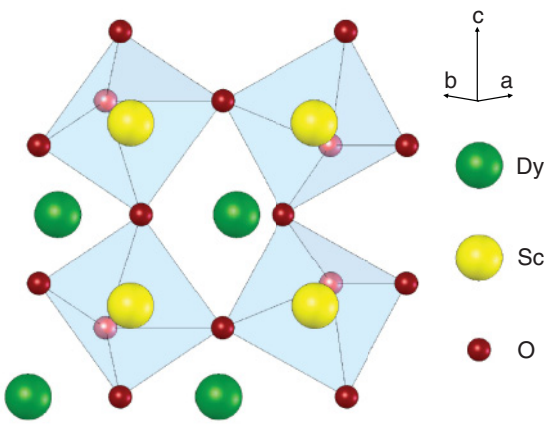

FIG. 1. (Color online) Top view of the crystal structure of a bulk (110) $DyScO_3$ unit cell, showing two atomic planes: ScO_2 on top and the DyO underneath.

surface morphology, RHEED on the surface crystal structure, and both SXRD and AR-MSRI give information on the chemical composition, crystal structure and roughness of the surface. As a consequence, these four different techniques will complement each other regarding the investigation of the surface structure. We used $DyScO_3$ as a model system. It has an orthorhombic crystal structure where $a = 0.5440$ nm, $b = 0.5717$ nm, and $c = 0.7903$ nm. The bulk oxygen octahedra are tilted, $a^+b^-b^-$ in Glazer's notation.[1,15]

Besides the singly terminated $DyScO_3$ surface, we have examined the surface at different stages of surface preparation. To understand possible structural reconstructions, we have compared our results with bulk $DyScO_3$ parameters, which are shown in Fig. 1 and Table I.

II. SUBSTRATE TREATMENT

Prior to the chemical treatment, as received $DyScO_3$ (110)[33] substrates are annealed at 1000 °C for 2 or 4 hours under a 150 mL/min O_2 flow. High-temperature annealing results in a redistribution of the atoms at the surface, giving well-defined step edges of approximately 0.2 and 0.4 nm. Note that increasing the annealing time straightens the terrace step edges. Subsequently, the $DyScO_3$ surfaces were chemically treated. It appeared that selective Dy etching by strong alkaline solutions occurs mainly at the step edges, which is comparable to wet etching of $SrTiO_3$ (001) and Si (111) surfaces.[17,18] As a result, the etching rate severely depended on the surface morphology, which varied from substrate to substrate, independent of the miscut angle. Therefore a surface

TABLE I. Fractional coordinates of bulk $DyScO_3$ [*Pbnm*(62) space group] at room temperature, as given by ICSD-99545 (see Ref. 16).

Atoms	*x*	*y*	*z*
Dy	0.0172	0.9393	0.2500
Sc	0.0000	0.5000	0.0000
O1	0.8804	0.5550	0.2500
O2	0.6926	0.3040	0.9392

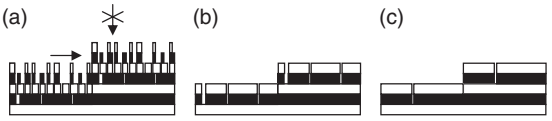

FIG. 2. Schematic cross section of the $DyScO_3$ (110) top layers, where black represents the DyO and white the ScO_2 planes. (a) After surface roughening (R), (b) after surface roughening and selective alkaline etching (RE), and (c) after selective alkaline etching (E). The arrows in (a) show schematically the selective etching process.

roughening step was introduced to increase the number of step edges. The effect of surface roughening is schematically depicted in Fig. 2(a). The roughening was done by acidic etching, as both the ScO as the DyO layers dissolve easily in acids, and reduced the minimum required selective etching time.[19,20]

To achieve surface roughening, $DyScO_3$ was immersed in water for 30 minutes and, subsequently, in buffered HF (NH_4F:HF = 87.5:12.5, pH = 5.5) for 30–60 seconds. Both steps were carried out in an ultrasonic bath. Thereafter, the substrates were rinsed with water (3×) and ethanol (1×). The selective alkaline etching, immersing in 12 M NaOH (aq) solution and, subsequently, in 1 M NaOH (aq) solution, was performed afterwards.[9] Both steps were carried out for 1 hour in an ultrasonic bath. Afterwards, the substrates were rinsed with water (3×) and ethanol (1×). AFM height images showing the surface morphology of differently treated substrates are given in Fig. 3. After each surface treatment step, the surface terrace structure is clearly visible; the height difference between the terraces corresponds to a single pseudocubic unit

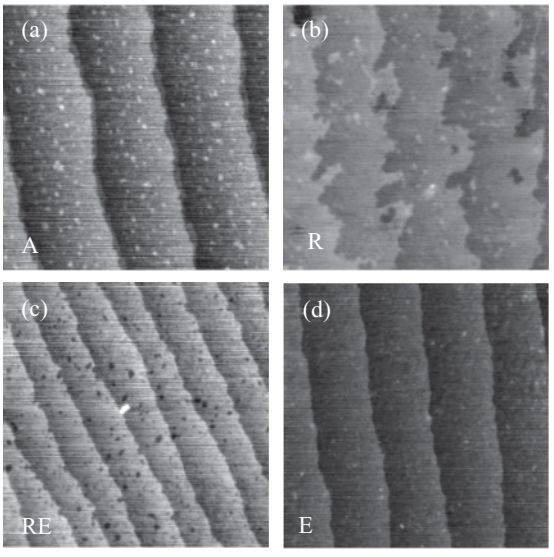

FIG. 3. AFM height images of differently treated $DyScO_3$ substrates. (a) Annealed for 2 hours at 1000 °C (a), followed by the surface roughening step (b). (c) Surface morphology after surface roughening and, subsequently, selectively etching. (d) Selective wet etched after annealing. The height difference between the terraces corresponds to a single pseudocubic unit cell (~0.4 nm). Small islands and holes are visible on the terraces. A, R, and E denote substrates after annealing, surface roughening step, and selective wet etching, respectively. All images are 1 × 1 μm^2.

cell (∼0.4 nm). Small islands and holes may be present on the terraces. For the mixed terminated surfaces, the islands and holes were 0.2 or 0.4 nm, while for the singly terminated surfaces only 0.4 nm holes and islands were observed. Single termination of selectively etched surfaces was confirmed by $SrRuO_3$ thin film growth, which is known to be sensitive to the surface termination and surface diffusivity.[9,21]

III. SURFACE ANALYSIS

Despite the fact that fully Sc-terminated $DyScO_3$ surfaces can be prepared, the surface structure of $DyScO_3$ is not well understood yet. A perfect, bulklike singly terminated surface is energetically unfavorable, due to its polar nature.

For each measurement technique, four samples at different stages of the surface treatment are discussed: after annealing (A), after annealing and surface roughening (R), after annealing and selective wet etching (E), and after annealing, surface roughening, and selective wet etching (RE). According to Kleibeuker *et al*., the first two samples, A and R, have a mixed terminated surface, which is in agreement with the observed $SrRuO_3$ island growth.[9] On the other hand, the samples E and RE are expected to be ScO_2 terminated.

A. RHEED

RHEED is a well-known technique to determine the primary in-plane surface structure periodicity of crystalline materials.[22] Insulating $DyScO_3$ easily charges in an electron beam at room temperature and high vacuum due to its large band gap (5.9 eV), complicating RHEED measurements.[2] Therefore the measurements were performed at 10^{-3} mbar O_2 to reduce surface charging. Figure 4 shows the diffraction patterns along the different $DyScO_3$ $(001)_{pc}$ surface directions, measured at room temperature using 30 keV electrons. The directions are indicated using two-dimensional direct lattice vectors, where the [01] or [10] direction corresponds to the orthorhombic [001] or $[1\bar{1}0]$ direction. No clear difference between the patterns along the [01] and [10] directions were observed, which implies fourfold symmetry.[34,35] By determining the size of the surface unit cell from the spacing of the diffraction spots, all diffraction patterns correspond to a bulk in-plane orthorhombic unit cell. No superstructure has been observed by RHEED. This suggests that possible reconstructions are within the unit cell, i.e., $DyScO_3$ has an (1 × 1) surface. Since Dy has a high atomic form factor, it has a large contribution to the RHEED pattern. As a result, possible variations between the differently treated substrates were not observed.

B. AR-MSRI

In order to determine the top-most atomic layer of $DyScO_3$ (110), we performed angle-resolved mass spectroscopy of recoiled ions (Ionwerks, Inc.). AR-MSRI is highly sensitive to surface composition with isotope resolution.[23] Since the exit velocity of recoiled elements is proportional to their mass, the resolution in time of flight can be converted to a resolution of atomic mass. Here, a time refocusing reflectron analyzer was used to increase the mass resolution. Note that the analyzer only detects the ionic fraction of the recoiled ions. The

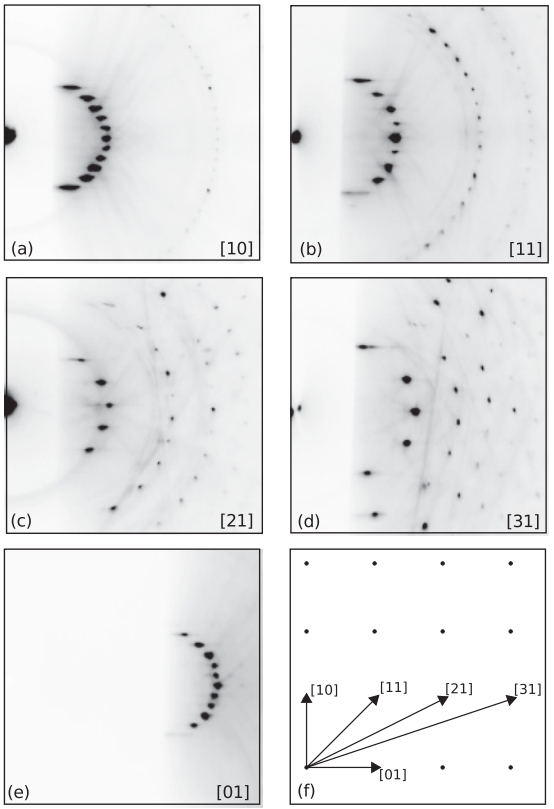

FIG. 4. RHEED patterns of an RE treated $DyScO_3$ surface along different directions: (a) along [10], (b) along [11], (c) along [21], (d) along [31], and (e) along [01]. (f) shows schematically the pseudocubic lattice structure, indicating the different directions.

number of recoiled ions is strongly influenced by neighboring ions at the surface due to blocking and/or shadowing effects. Therefore systematic investigations on the dependence of the mass spectroscopy of recoiled ions counts versus azimuthal angle (δ) can give information on the in-plane crystalline structures.[11,23]

Before the AR-MSRI measurements, the samples were cleaned in acetone and isopropanol in turn (in an ultrasonic bath). In the high-vacuum AR-MSRI chamber, the samples were heated to 600 °C in 7×10^{-2} mbar O_2 to remove hydrocarbons from the substrate. For the measurements, pulsed potassium ions ^{39}K with kinetic energy of 10 keV are directed to the surface of the samples at an incident angle of 15°, and recoiled ions from the sample are collected at a recoil angle of 60° by the reflectron analyzer. The measurements were performed at 150 °C in high vacuum (below 10^{-6} mbar). Note that $DyScO_3$ has no structural phase transitions between room temperature and 150 °C.[24]

Full range mass spectra were collected of the four different samples at different azimuthal angles and normalized with respect to the integrated intensity of the K peak. The Sc/Dy intensity ratios as a function of the azimuthal angle of the four samples are shown in Fig. 5. For the singly (RE and E) terminated samples, maxima at −45° and 45° are well pronounced. This is due to shadowing of Dy by the topmost Sc and O atoms. This can only be observed when the surface is mainly ScO_2 terminated. The as received substrate shows

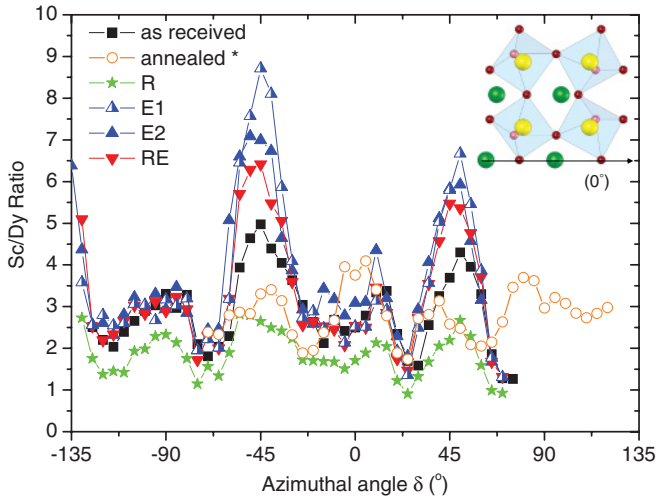

FIG. 5. (Color online) Azimuthal maps of differently treated $DyScO_3$ (110) substrates: as-received, after surface roughening (R), after selective etching (E), and after surface roughening plus selective etching (RE). The data of annealed $DyScO_3$, indicated by *, were taken from Kleibeuker *et al.*[9] Maximum blocking of Dy was observed at $-45°$ and $45°$. The inset shows the top view shown in Fig. 1. The arrow indicates $0°$ azimuthal angle.

small maxima at $-45°$ and $45°$, suggesting a Sc rich surface. However, Dy blocking by O atoms may induce an increased Sc/Dy ratio as well. After annealing as well as after the surface roughening step, the $DyScO_3$ surfaces are clearly mixed terminated. This is in agreement with our etching model as well as the observed $SrRuO_3$ island growth.

When comparing the E samples and the RE sample, only small differences were observed. This may be due to difference in surface roughness and would be in agreement with the AFM height analysis. Note that E1 and E2 were treated equally, but E1 has a slightly lower surface roughness than E2, determined by AFM. Increase of the surface roughness broadens the structure in the recoiled features.[25] However, the angular resolution of our setup is not sufficient to measure this broadening. Despite the suitability of AR-MSRI to determine the dominant termination layer, the ability to prove perfect single termination can be compromised by surface roughness.

Therefore no clear differences in AR-MSRI spectra between the RE and E samples are observed. From the AR-MSRI data, it can be concluded that both samples are predominantly ScO_2 terminated. The possible presence of a small Dy fraction at the surface is hard to establish.

The AR-MSRI data show a fourfold rotation symmetry, since Sc blocks Dy every $90°$. This is in agreement with our RHEED data. Small variations between $-45°$ and $45°$ may be due to the orthorhombic crystal structure. The measurements are not accurate enough to determine slight deviations in the angle. The weak features at other angles may be due to the contribution of oxygen.

C. Surface x-ray diffraction

SXRD is a well established technique to obtain structural information on crystal surfaces. It is based on the accurate determination of the intensity of the crystal truncation rods (CTR). CTRs arises due to the abrupt truncation of the crystal by its surface. The CTRs are lines, in reciprocal space, perpendicular to the surface plane and interconnecting bulk Bragg peaks.[26–28]

As the CTR profile depends sensitively on the atomic structure arrangement at the surface, it is a very useful tool to provide structural information. The crystallographic directions are chosen such that h and k lie in the surface plane, while l is in the direction perpendicular to the surface. The scattering amplitude is given by the coherent sum of the scattering arising from the bulk and the surface layer.

Using the bulk atomic positions of $DyScO_3$ (see Table I) and transforming them to the (110) surface setting, the alternating layered structure (ScO_2 and DyO planes) is obtained and used as a starting point for the models presented. For simplicity, the atomic positions were fixed at their bulk position in all the models. The data were fitted by varying the occupancy of each atomic plane, creating different models like singly or mixed terminated surfaces. It has to be mentioned that from the model, a perfect ScO_2 terminated surface results in the same CTRs as a perfect DyO terminated surface. Only when deviations from a perfect singly terminated surface, e.g., holes or mixed termination, are included, the difference between the two terminations can be observed. Both cations and oxygen are contributing to each CTR owing to the symmetry of the $DyScO_3$ unit cell.

The SXRD measurements were done using the $(2+3)$ axis diffractometer on the BM26 (DUBBLE) beamline at the ESRF (Grenoble, France) at an energy of 16 keV.[29] The substrates were heated to 250 °C under a constant flow of dry nitrogen in order to eliminate the influence of adsorbed water at the surface. The recorded data were processed and analyzed with the ANA-ROD package, using normalized χ^2 as goodness-of-fit criterion for the models presented.[30] For each sample, a minimum of 6 CTRs plus the specular rod were measured. By scanning reciprocal space with radial scans, no fractional order reflections were found. This indicates that the surface is unreconstructed, which is in agreement with the RHEED measurements.

A selection of the CTRs for all four samples is shown in Fig. 6. Comparing the A and R samples with E and RE samples, clear differences are observed. For surfaces with A and R treatment, the data (A open circles, R black circles) do not match the single termination model (dashed curve).

The data of the roughened surfaces (R) were fitted with a simple surface model, optimizing the occupancy of the top four atomic planes ($2\times$ ScO_2, $2\times$ DyO), yielding a reasonable fit (black solid line) for the data of the R sample. Adding more layers to the model does not improve the fit significantly. A schematic representation of the surface model of the fit results is shown in Fig. 2(a) and the optimized occupancies are listed in Table II. The same model was used to fit the data of the A sample, resulting in slightly different occupancies of the four layers. Taking into account the simplicity of the model, the model results in reasonable fits. Using more sophisticated models, taking into account atomic displacements and thermal vibrations other than bulk values within the top layers, is expected to yield a better fit.[31]

On the other hand, the rods of E and RE [see Figs. 6(c) and 6(d)] could be well fitted with a perfect ScO_2 terminated

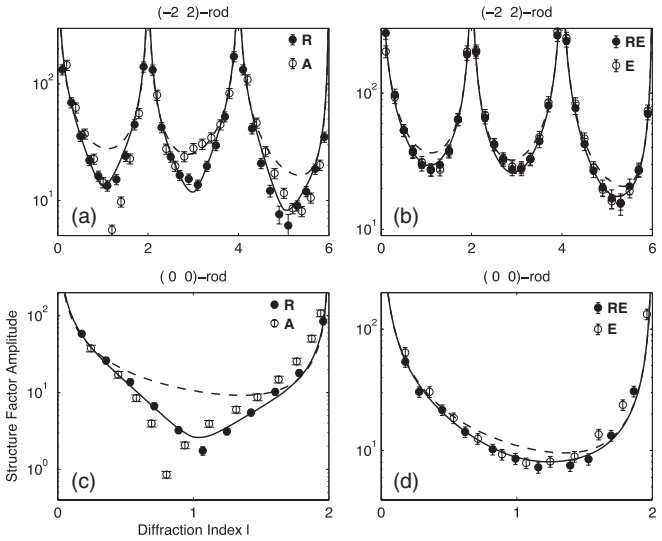

FIG. 6. The (−2 2) and (0 0) crystal truncation rods of $DyScO_3$ after annealing (A, open circles) and surface roughening (R, filled circles) in (a) and (c) and after selective etching (E, open circles) and both surface roughening and selective etching (RE, filled circles) in (b) and (d). The dashed curves show the fits to a perfect ScO_2 terminated surface. The solid curves are the fits to the data of R (a and c) and RE (b and d) treated $DyScO_3$ (see text).

surface (dashed line, $\chi^2 = 2.9$). The fit can be improved by reducing the occupancy of the two topmost planes by 10% (solid black line, $\chi^2 = 2.3$ for RE). This is in full agreement with the AFM image of RE, showing a similar amount of 0.4 nm holes on the step terraces [see Fig. 3(c)]. Schematic representations of the surface model of the fit results for RE and E are shown in Fig. 2(b) and 2(c). Increasing the percentage of holes to 20% does not improve the fit ($\chi^2 = 2.7$), nor does a DyO terminated surface with a 10% reduced occupancy of the two topmost planes ($\chi^2 = 2.9$). Also modeling a ScO_2 terminated surface with a partially occupied layer of DyO on top, does not yield a better fit (e.g., 5% DyO, $\chi^2 = 2.6$). The results are listed in Table II.

Using SXRD, we show that unreconstructed, ScO_2 terminated surfaces were achieved for the E and RE treated samples.

TABLE II. The normalized χ^2 of several models on the different treated $DyScO_3$ surfaces. The occupancies of the top four atomic surface layers are given, where DyO (2) is the most bulk like and ScO_2 (1) is the top most atomic plane.

	Occupancy				
Best model	DyO (2)	ScO_2(2)	DyO (1)	ScO_2 (1)	χ^2
R	0.74	0.60	0.28	0.12	3.6
A	0.91	0.63	0.42	0.36	3.8
E	1.00	1.00	0.90	0.90	2.5
RE	1.00	1.00	0.90	0.90	2.3
Alternative models					
RE	1.00	1.00	1.00	1.00	2.9
RE	1.00	1.00	0.80	0.80	2.7
RE	1.00	1.00	0.05	0.00	2.6
RE	1.00	0.90	0.90	0.00	2.9

There is no indication for a deficiency of cations at the surface. Due to the relatively low atomic number of oxygen, SXRD is not sufficiently sensitive to detect possible oxygen vacancies. The A and R treatment resulted in mixed terminated and rough surfaces. This is in agreement with our etching model, AR-MSRI data and $SrRuO_3$ island growth results.

IV. DISCUSSION

SXRD as well as AR-MSRI measurements showed that Sc is the dominant cation at the surface of both E and RE samples. $SrRuO_3$ thin film growth confirmed single termination of the RE samples, while for the E samples the termination varied from singly terminated to nearly singly terminated. The RE samples appeared to have an increased number of step edges, which was observed by AFM, AR-MSRI and SXRD. The increased number of step edges is due to the nonselective buffered HF etching. This also explains the roughened terrace step edges for sample R in comparison to sample A [see Figs. 3(a) and 3(b)].

Our RHEED data show an (1 × 1) surface for $DyScO_3$ (110). The fourfold symmetry is also confirmed by AR-MSRI, as it shows clear maxima every 90°. Moreover, the used model to fit the CTRs suggests that cation displacements are negligible. This implies that the cation surface structure is unreconstructed. However, the precise stoichiometry of the surface layer has not yet been determined. The structure is such that vacancies in the surface layer are compatible with an (1 × 1) diffraction pattern. Therefore, ordered cation vacancies are unlikely to occur.

Oxygen vacancies at the surface of ScO_2 terminated $DyScO_3$ reduce the total charge. Inserting one oxygen vacancy per orthorhombic in-plane unit cell at the surface, the charge of the scandium oxide plane is halved. This would be sufficient to overcome the polar discontinuity between bulk $DyScO_3$ and vacuum. Moreover, adsorbates are present when $DyScO_3$ is exposed to air and may also play a role in avoiding the polar discontinuity. It has to be mentioned that the techniques presented in this paper are not sufficiently sensitive to determine the presence and role of oxygen vacancies and adsorbates at the $DyScO_3$ (110) surface.

Here, we have studied mixed and ScO_2 terminated $DyScO_3$ surfaces. The next step will be switching the surface termination to Dy. This may be achieved by depositing a monolayer of DyO on top of a ScO_2 terminated $DyScO_3$. This is similar to SrO deposition on Ti terminated $SrTiO_3$.[32] Note that on Dy terminated surfaces, oxygen vacancies are unlikely to occur, since the surface is positively charged.

V. CONCLUSION

We have shown that selectively etched $DyScO_3$ substrates have a (1 × 1) reconstructed ScO_2 terminated surface. This points to the absence of ordered cation vacancies at the surface. Moreover, our SXRD data indicate that cation displacements in relation to the bulk atomic planes are unlikely to be present. Therefore we suggest that the polarity difference between bulk and vacuum is most likely overcome by introducing oxygen vacancies in the topmost ScO_2 layer or by the presence of adsorbates. These results are important for the understanding

of polar perovskite-type oxide surfaces and thin film growth on these surfaces.

ACKNOWLEDGMENTS

G. R. thanks the financial support by The Netherlands Organization for Scientific Research (NWO) through a VIDI grant. W. S. acknowledges support by the U.S. Department of Energy, Office of Basic Science, Materials Sciences and Engineering Division. J. R. acknowledges the support from the Link Foundation. P. T. and S. H. acknowledge the financial support of NWO for the measurements at DUBBLE (ESRF).

*g.koster@utwente.nl

[1] R. Uecker, B. Veličkov, D. Klimm, R. Bertram, M. Bernhagen, M. Rabe, M. Albrecht, R. Fornari, and D. G. Schlom, J. Cryst. Growth **310**, 2649 (2008).
[2] M. Raekers, K. Kuepper, S. Bartkowski, M. Prinz, A. V. Postnikov, K. Potzger, S. Zhou, A. Arulraj, N. Stüßer, R. Uecker, W. L. Yang, and M. Neumann, Phys. Rev. B **79**, 125114 (2009).
[3] D. G. Schlom, L.-Q. Chen, C.-B. Eom, K. M. Rabe, S. K. Streiffer, and J.-M. Triscone, Annu. Rev. Mater. Res. **37**, 589 (2007).
[4] S. J. May, J. W. Kim, J. M. Rondinelli, E. Karapetrova, N. A. Spaldin, A. Bhattacharya, and P. J. Ryan, Phys. Rev. B **82**, 014110 (2010).
[5] J. He, A. Borisevich, S. V. Kalinin, S. J. Pennycook, and S. T. Pantelides, Phys. Rev. Lett. **105**, 227203 (2010).
[6] K. J. Choi *et al.*, Science **306**, 1005 (2004).
[7] M. Kawasaki, K. Takahashi, T. Maeda, R. Tsuchiya, M. Shinohara, O. Ishiyama, T. Yonezawa, M. Yoshimoto, and H. Koinuma, Science **266**, 1540 (1994).
[8] G. Koster, B. L. Kropman, G. J. H. M. Rijnders, D. H. A. Blank, and H. Rogalla, Appl. Phys. Lett. **73**, 2920 (1998).
[9] J. E. Kleibeuker *et al.*, Adv. Funct. Mater. **20**, 3490 (2010).
[10] J. L. Blok, X. Wan, G. Koster, D. H. A. Blank, and G. Rijnders, Appl. Phys. Lett. **99**, 151917 (2011).
[11] A. Biswas, P. B. Rossen, C.-H. Yang, W. Siemons, M.-H. Jung, I. K. Yang, R. Ramesh, and Y. H. Jeong, Appl. Phys. Lett. **98**, 051904 (2011).
[12] R. J. Francis, S. C. Moss, and A. J. Jacobson, Phys. Rev. B **64**, 235425 (2001).
[13] C. Noguera, J. Phys.: Condens. Matter **12**, R367 (2000).
[14] E. Heifets, W. A. Goddard III, E. A. Kotomin, R. I. Eglitis, and G. Borstel, Phys. Rev. B **69**, 035408 (2004).
[15] J. Schubert, O. Trithaveesak, A. Petraru, C. L. Jia, R. Uecker, P. Reiche, and D. G. Schlom, Appl. Phys. Lett. **82**, 3460 (2003).
[16] R. P. Liferovich and R. H. Mitchell, J. Solid State Chem. **177**, 2188 (2004).
[17] J. Broekmaat, Ph.D. thesis, University of Twente, 2008.
[18] P. Jakob and Y. J. Chabal, J. Chem. Phys. **95**, 2897 (1991).
[19] D. Lide, *CRC Handbook of Chemistry and Physics CD-ROM Version 2010* (Taylor and Francis, FL, 2009).
[20] L. Pauling, *The Nature of the Chemical Bond*, 3rd ed. (Cornell University press, NY, 1960).
[21] B. Kuiper, J. L. Blok, H. J. W. Zandvliet, D. H. A. Blank, G. Rijnders, and G. Koster, MRS Communications **1**, 17 (2011).
[22] G. Koster and G. Rijnders, *In Situ Characterization of Thin Film Growth* (Woodhead Publishing, Cambridge, UK, 2012).
[23] J. Rabalais, *Principles and Applications of Ion Scattering Spectrometry: Surface Chemical and Structural Analysis* (Wiley-Interscience, NJ, 2003).
[24] M. D. Biegalski, J. H. Haeni, S. Trolier-McKinstry, D. G. Schlom, C. D. Brandle, and A. J. Ven Graitis, J. Mater. Res. **20**, 952 (2005).
[25] A. Gozar, G. Logvenov, V. Y. Butko, and I. Bozovic, Phys. Rev. B **75**, 201402(R) (2007).
[26] I. K. Robinson, Phys. Rev. B **33**, 3830 (1986).
[27] R. Feidenhans'l, Surf. Sci. Rep. **10**, 105 (1989).
[28] E. Vlieg, Surf. Sci. **500**, 458 (2002).
[29] E. Vlieg, J. Appl. Crystallogr. **31**, 198 (1998).
[30] E. Vlieg, J. Appl. Crystallogr. **33**, 401 (2000).
[31] P. Tinnemans, S. Harkema, H. Graafsma, A. Janssens, G. Portale, and E. Vlieg (unpublished).
[32] A. Ohtomo and H. Y. Hwang, Nature (London) **427**, 423 (2004).
[33] The orthorhombic (110) corresponds to the cubic (100).
[34] For the measurement along the [01] direction, the direct beam was not present in the RHEED pattern as it was blocked by the sample holder.
[35] Note that small differences between the [10] and [01] direction are expected as they are different in bulk $DyScO_3$. However, the differences are too small to be determined accurately by RHEED.